SERBIAN JOURNAL OF ELECTRICAL ENGINEERING
Vol. 5, No. 1, May 2008, 109-120

Frequency Domain Analysis of Lightning Protection Using Four Lightning Protection Rods

Vesna Javor[1], Predrag Rancic[2]

Abstract: In this paper the lightning discharge channel is modelled as a vertical monopole antenna excited by a pulse generator at its base. The lightning electromagnetic field of a nearby lightning discharge in the case of lightning protection using four vertical lightning protection rods was determined in the frequency domain. Unknown current distributions were determined by numerical solving of a system of integral equations of two potentials using the Point Matching Method and polynomial approximation of the current distributions. The influence of the real ground, treated as homogeneous loss half-space of known electrical parameters, expressed through a Sommerfeld integral kernel, was modeled using a new Two-image approximation which gives good results in both near and far fields.

Keywords: Lightning electromagnetic field, Vertical monopole antenna, Lightning protection rod, Sommerfeld integral.

1 Introduction

A vertical mast antenna (VMA), excited by a pulse generator at its base, is often used for calculating the lightning radiated electromagnetic field as a model of lightning discharge channel of the return stroke [1] with the supposed channel base current at the striking point (e.g. [2] and [3]). The lightning electromagnetic field (LEMF) from the current distribution along the channel is determined in the time domain using the antenna theory whereas the ground is usually treated as a perfectly conducting half-space [4]. Real ground influence is included in calculations in the frequency domain (e.g. [5]) and then an Inverse Fourier Transform is used for obtaining results in the time domain. If the ground is treated as a homogeneous loss half-space, then the Sommerfeld integral [6] including ground electrical characteristics and system geometry parameters has to be solved. Several approximations of the Sommerfeld integral kernel have been proposed in literature in order to solve the integral numerically. One of those is

[1] Faculty of Electronic Engineering of Nis, Department of Theoretical Electrical Engineering, Ul. Aleksandra Medvedeva 14, 18 000 Nis, Serbia, e-mail: vjavor@elfak.ni.ac.yu
[2] Faculty of Electronic Engineering of Nis, Department of Power Engineering, Ul. Aleksandra Medvedeva 14, 18 000 Nis, Serbia, e-mail: prancic@elfak.ni.ac.yu

the new Two image approximation (TIA) [7] of the Sommerfeld integral kernel that gives good results in the near and far field zone as well ([8-10]).

In this paper VMA and vertical lightning protection rods (LPRs) are treated as a unique problem for boundary conditions. Unknown current distributions along VMA and LPRs were determined from the SIE-TP [11] using the Point matching method as the Method of Moments (MoM) [12] and polynomial approximation for the current distributions [13]. Counter-poises of the antenna and protection rods, i.e. their contacts to the ground, are adopted as semi-spherical grounding electrodes equivalent to concrete mast foundations ([14]).

Input impedances of VMA with four LPRs in the surroundings and grounding impedances for different LHS electrical parameters are determined, as integral characteristics of the presented system, confirming the accuracy of EMF calculations. Results of Sommerfeld integral kernel calculations for different distances from VMA confirm the TIA accuracy in both near and far fields. The results are compared to the results of other authors [15] and their programs [16].

In this way the LEMF is modeled in the frequency domain and a Fourier transform application can be carried out for determining LEMF in the time domain.

2 Theoretical Background

The lightning discharge channel is modelled by VMA having a total height $h = l_1 + l_2 + \cdots + l_N$ and circular cross section of radius a, $a << l_k$, $a << \lambda_0$, $k = 1,2,\ldots,N$ (λ_0 - the wavelength in the air). VMA is in the vicinity of four LPRs placed on a square at ground level. LPR heights are h_p, $h_p = l_{N+p}$, radii a_p, $a_p << h_p$, and $a_p << \lambda_0$, p = 1, 2, 3 and 4, positioned as in Fig. 1.

VMA is energized at its base by an ideal generator of voltage $U = 1\text{V}$ and frequency *f*. Counter-poises of VMA and LPRs are small semi-spherical grounding electrodes of radii a_{gk}, $a_{gk} << \lambda_0$, $k = 1,2,\ldots,5$ which replace their contacts to the ground. The influence of grounding electrode currents on the electromagnetic field in air is modelled with the field of vertical Hertz dipoles of moments $p_{gk} = I(0^-)\, a_{gk}$ placed immediately below the ground surface (Fig. 1).

The surrounding ground is modelled by linear isotropic and homogeneous loss half-space of known electrical parameters: σ_1 - specific conductivity, $\varepsilon_1 = \varepsilon_0 \varepsilon_{r1}$ - electric permittivity and $\mu_1 = \mu_0$ - magnetic permeability. Other parameters of two half-spaces (for $i = 0,1$) are denoted as: $\underline{\sigma}_i = \sigma_i + \mathrm{j}\omega\varepsilon_i$ - complex conductivity, $\underline{\gamma}_i = (\mathrm{j}\omega\mu_i \underline{\sigma}_i)^{1/2}$ - complex propagation constant,

$\underline{n}_{10} = \underline{\gamma}_1 / \underline{\gamma}_0$ - refraction index, $\underline{\varepsilon}_{r1} = \varepsilon_{r1} - \mathrm{j}\varepsilon_{i1} = \varepsilon_{r1} - \mathrm{j}60\sigma_1\lambda_0$ - complex relative permittivity, and $\omega = 2\pi f$ - angular frequency. Unknown current distributions, localized along axes of VMA and LPRs, are denoted as $I'_k(s'_k)$, $k = 1,2,...,N+4,$ where $k = N + p$ denotes current along *p*-th LPR. The degree of the polynomial approximation for the *k*-th segment current is n_k.

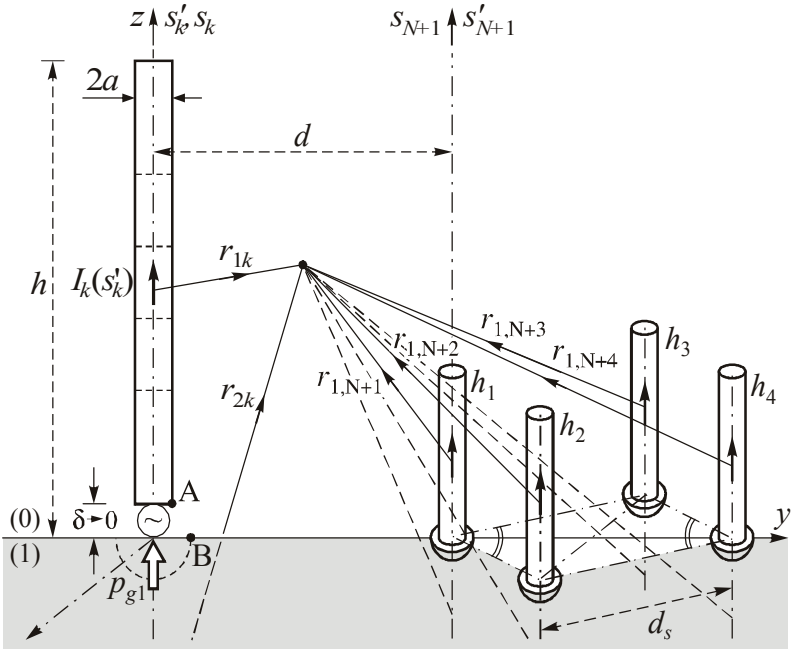

Fig. 1 – *Lightning discharge channel modelled by* VMA *in the vicinity of four* LPRs.

The Hertz vector potential, $\vec{\Pi}_0 = \Pi_{z0}(s)\hat{z}$, and electric scalar potential, $\varphi_0(s) = -\mathrm{div}\vec{\Pi}_0 = -\partial\Pi_{z0}/\partial z$, calculated at conductor surfaces as functions of local coordinate *s*, $0 \le s \le s_n \le l_n$, $n = 1,2,\ldots N+4$, satisfy the SIE-TP and they are given with the following expressions:

$$\Pi_{z0}(s) = \frac{1}{4\pi\underline{\sigma}_0}\left\{\sum_{k=1}^{N+4}\int_{s_k'=0}^{l_k} I_k(s_k')[K_0(r_{1k}) + S_{00}^{v}(r_{2k})]\mathrm{d}s'_k + \right.$$
$$\left. + (\delta_{1k} + \sum_{p=1}^{4}\delta_{N+p,k})\, p_{gk}\, S_{01}^{v}(r_{2k}, s'_k = 0)\right\}, \qquad (1)$$

$$\varphi_0(s)=\frac{1}{4\pi\underline{\sigma}_0}\left\{\sum_{k=1}^{N+4}\int_{s_k'=0}^{l_k} I_k(s_k')\frac{\partial}{\partial s_k'}[K_0(r_{1k})-S_{00}^v(r_{2k})]\mathrm{d}s_k' - \right.$$
$$\left. -(\delta_{1k}+\sum_{p=1}^{4}\delta_{N+p,k})\,p_{gk}\frac{\partial}{\partial z}S_{01}^v(r_{2k},s_k'=0)\right\} \tag{2}$$

for k referring to the k-th segment, $K_0(r_{jk})=\exp(-\underline{\gamma}_0 r_{jk})/r_{jk}$ - the standard potential kernel, $j=1$ for the current elements along VMA, $j=2$ and 3 for the image current elements below the ground, $S_{00}^v(r_{2k})$ - Sommerfeld integral kernel of the image current element; δ_{1k} and $\delta_{N+p,k}$ - Kronecker's symbols; and $S_{01}^v(r_{2k},s_k'=0)$ - Sommerfeld integral kernel of the Hertz dipole counter-poise,

$$S_{01}^v(r_{2k},s_k'=0)=\underline{n}_{10}^{-2}[K_0(r_{2k})+S_{00}^v(r_{2k})]. \tag{3}$$

Using the new Two-image approximation of the Sommerfeld integral kernel in (1)-(3), the following is obtained:

$$S_{00}^v(r_{2k})\cong BK_0(r_{2k})+A\exp(\underline{\gamma}_0 d_{im})K_0(r_{3k}), \tag{4}$$

for $B=R_\infty$, $A=R_0-R_\infty$, $R_\infty=(\underline{n}_{10}^2-1)/(\underline{n}_{10}^2+1)$, $R_0=(\underline{n}_{10}-1)/(\underline{n}_{10}+1)$, $d_{im}=\left|\underline{\gamma}_0^{-1}(1+\underline{n}_{10}^{-2})\right|$, and the distance r_{3k} from the second image to the field point is $r_{3k}=\sqrt{\rho^2+(z+z_k'+d_{im})^2}$.

Using this procedure and numerical solving of the SIE-TP the current distributions are determined, and afterwards the input and grounding impedances are calculated as:

$$Z_{in}=R_{in}+\mathrm{j}X_{in}=\frac{U}{I_1(s_1'=0)}=Z_a+Z_g, \tag{5}$$

$$Z_a=R_a+\mathrm{j}X_a=\frac{\varphi_0(s_1=0^+)}{I_1(s'_1=0)}, \tag{6}$$

$$Z_g=-\frac{\varphi_0(s_1=0^-)}{I_1(s'_1=0)}=-\frac{\varphi_0(s_1=0^-)}{U}Z_{in}, \tag{7}$$

for Z_a - the input impedance referred to electric scalar potential of point A.

3 Numerical Results

Numerical results presented in the following tables illustrate the convergence of the input impedance for a different number of segments along VMA and LPRs and for a different polynomial degree in the current distribution approximation, as one of the validation parameters of the whole method.

For ground parameters $\varepsilon_{r1}=10$ and $\sigma_1\lambda_0=1\mathrm{S}$ the results for the input impedance of a single VMA of height $h=0.25\lambda_0$ and radius $a=0.0005\lambda_0$ are presented in **Table 1**, for a different number of segments *N* and different polynomial degree n_k along each segment. For the VMA-LPRs system of parameters $h=h_p=0.25\lambda_0$, $a=a_p=0.0005\lambda_0$, $p=1,2,3,4$, $\beta_0 d=5$, the results for Z_a are presented in **Table 2**, for a different polynomial degree n_k, $k=1,...,N+4$, and different number of segments *N* (along VMA) equal to the number of segments N_p (along LPRs). The LPRs are square positioned as in Fig. 1 and the square edge is of the length $d_s=0.25\lambda_0$.

For the single VMA of height $h=0.5\lambda_0$ the results for Z_a are presented in **Table 3**, and for a VMA-LPRs system in **Table 4**, for $N_p=1$, $p=1,2,3,4$, different number of segments *N* (along VMA) and different polynomial degree n_k, $k=1,...,N+4$. For the same parameters, but $h=\lambda_0$, the results for Z_a are presented in **Tables 5** and **6**. On the basis of the presented convergence of the results for Z_a it can be concluded that the used method is properly realized, because the input impedance presents a integral characteristic of the system. Modulus of current distribution as the function of a normalized distance along the *s*' axis is presented in Fig. 2 for the VMA, and in Fig. 3 for the four LPRs, for the following system parameters: $h=0.5\lambda_0$, $h_p=0.25\lambda_0$, $a=a_p=0.0005\lambda_0$, $N=1$, $N_p=1$, $p=1,2,3,4$ and $n_k=4$, $k=1,...,5$. The normalized distance between VMA and the nearest LPR of the square positioned LPRs is taken as parameter $\beta_0 d=2,\ 5$ and 10. The results for current distributions in the case of VMA having a height of $h=\lambda_0$, $N=4$, and LPRs of $h_p=0.25\lambda_0$, $a=a_p=0.0005\lambda_0$, $N_p=1$, $p=1,2,3,4$, and $n_k=4$, $k=1,...,8$, are presented in Figs. 4 and 5, for normalized distance as the parameter.

The results for electric field values along the radial direction coinciding with the y^+-axis, for $z=0$ and $\beta_0\rho\in[0.1\div500]$ are presented in Figs. 6 and 7. The spikes correspond to the nearest and the farthest LPRs.

Table 1

Input impedance of a single VMA *for* $h = 0.25\lambda_0$ *and* $a = 0.0005\lambda_0$, *for ground parameters* $\varepsilon_{r1} = 10$ *and* $\sigma_1\lambda_0 = 1\text{S}$.

N	$Z_a = R_a + \text{j}X_a$ in Ω		
	$n_k = 2$	$n_k = 3$	$n_k = 4$
1	39.16+j21.05	38.98+j20.57	39.40+j20.69
2	39.01+j20.87	39.32+j20.96	39.48+j21.09
4	39.28+j21.03	39.57+j21.19	39.72+j21.25
10	39.62+j21.27	39.85+j21.30	40.00+j21.24

Table 2

Input impedance of VMA-LPRs *for* $h = h_p = 0.25\lambda_0$, $a = a_p = 0.0005\lambda_0$, $N = N_p$, $p = 1,\ldots,4$, $\beta_0 d = 5$, *for ground parameters* $\varepsilon_{r1} = 10$ *and* $\sigma_1\lambda_0 = 1\text{S}$.

N	$Z_a = R_a + \text{j}X_a$ in Ω		
	$n_k = 2$	$n_k = 3$	$n_k = 4$
1	40.77+j23.10	40.54+j22.63	40.96+j22.72
2	40.72+j23.00	41.07+j23.06	41.26+j23.18
4	41.63+j23.33	42.31+j23.41	42.53+j23.46

Table 3

Input impedance of a single VMA *for* $h = 0.5\lambda_0$ *and* $a = 0.0005\lambda_0$, *for ground parameters* $\varepsilon_{r1} = 10$ *and* $\sigma_1\lambda_0 = 1\text{S}$.

N	$Z_a = R_a + \text{j}X_a$ in Ω		
	$n_k = 2$	$n_k = 3$	$n_k = 4$
1	604.30-j695.40	603.19-j707.02	620.21-j710.71
2	593.22-j697.81	615.10-j709.25	598.85-j705.19
4	619.76-j710.07	586.40-j702.50	565.95-j698.75
8	587.80-j702.87	557.34-j697.23	538.65-j693.94

Table 4

Input impedance of VMA-LPRs *for* $h = 2h_p = 0.5\lambda_0$, $a = a_p = 0.0005\lambda_0$, $N_p = 1$, p=1,..., 4, $\beta_0 d = 5$, *for ground parameters* $\varepsilon_{r1} = 10$ *and* $\sigma_1\lambda_0 = 1\text{S}$.

N	$Z_a = R_a + \text{j}X_a$ in Ω		
	$n_k = 2$	$n_k = 3$	$n_k = 4$
1	569.21-j675.74	567.85-j687.36	583.40-j691.25
2	560.44-j676.49	580.20-j687.83	565.26-j683.54
4	605.17-j696.03	571.54-j687.05	553.09-j684.39

Table 5

Input impedance of a single VMA *for* $h = \lambda_0$ *and* $a = 0.0005\,\lambda_0$, *for ground parameters* $\varepsilon_{r1} = 10$ *and* $\sigma_1 \lambda_0 = 1\text{S}$.

N	$Z_a = R_a + \mathrm{j}X_a$ in Ω		
	$n_k = 2$	$n_k = 3$	$n_k = 4$
2	614.00-j510.78	569.45-j569.11	605.61-j581.48
4	599.42-j578.01	587.18-j576.40	571.69-j575.87
8	582.18-j577.00	561.85-j575.42	546.47-j575.11

Table 6

Input impedance of VMA-LPRs *for* $h = 4h_p = \lambda_0$, $a = a_p = 0.0005\,\lambda_0$, $N_p = 1$, $p = 1, \ldots, 4$, $\beta_0 d = 5$, *for ground parameters* $\varepsilon_{r1} = 10$ *and* $\sigma_1 \lambda_0 = 1\text{S}$.

N	$Z_a = R_a + \mathrm{j}X_a$ in Ω		
	$n_k = 2$	$n_k = 3$	$n_k = 4$
2	590.03-j523.14	542.43-j581.35	579.12-j593.87
4	569.68-j588.14	557.83-j585.86	542.91-j584.26
8	566.91-j574.89	545.78-j571.50	532.02-j572.12

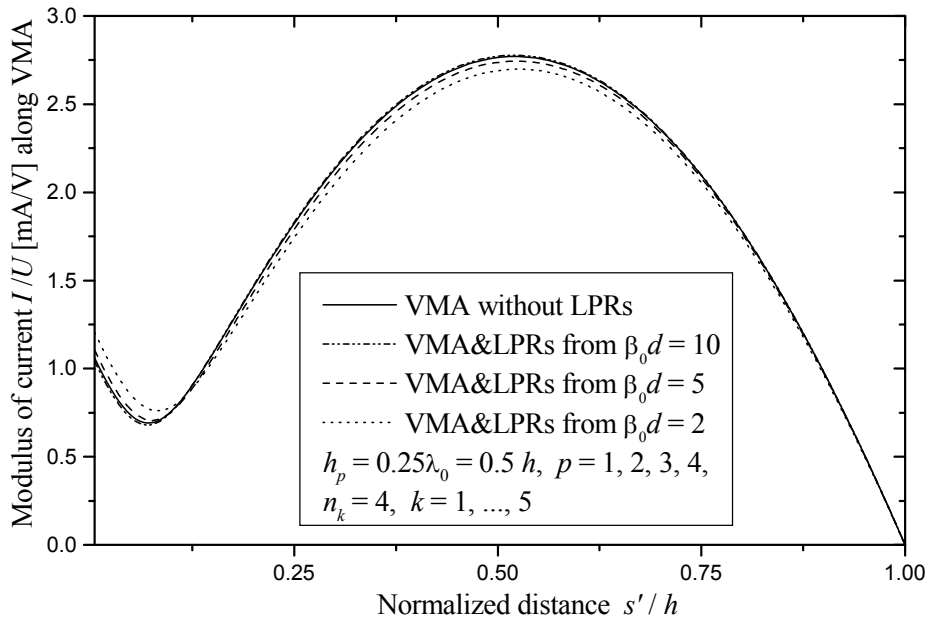

Fig. 2 – *Modulus of I*/*U along* VMA, *for* $h = 0.5\,\lambda_0$.

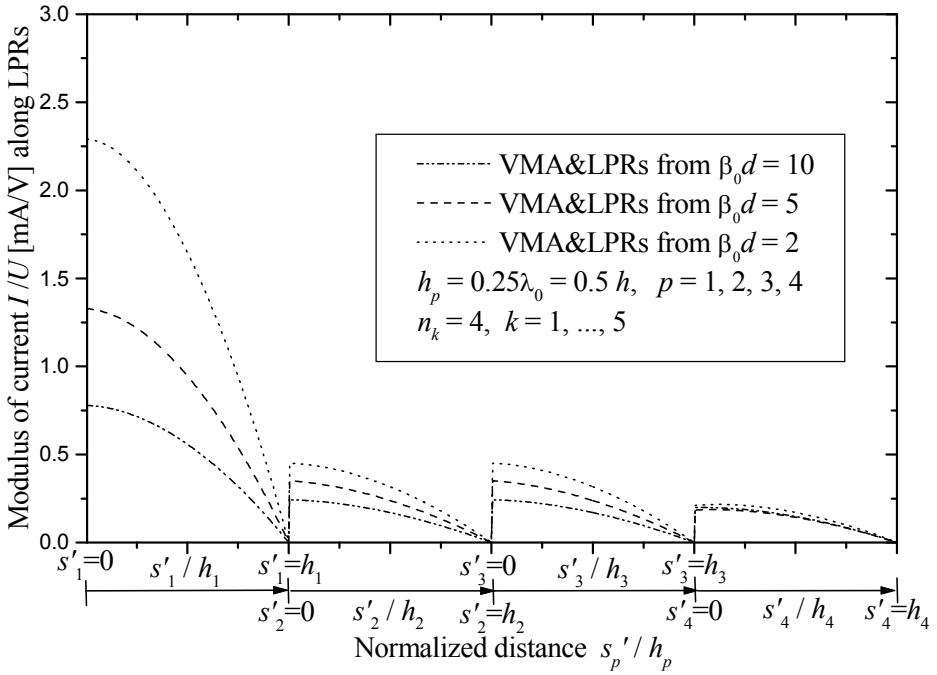

Fig. 3 – *Modulus of* I/U *along* LPRs, *for* $h = 0.5\lambda_0$.

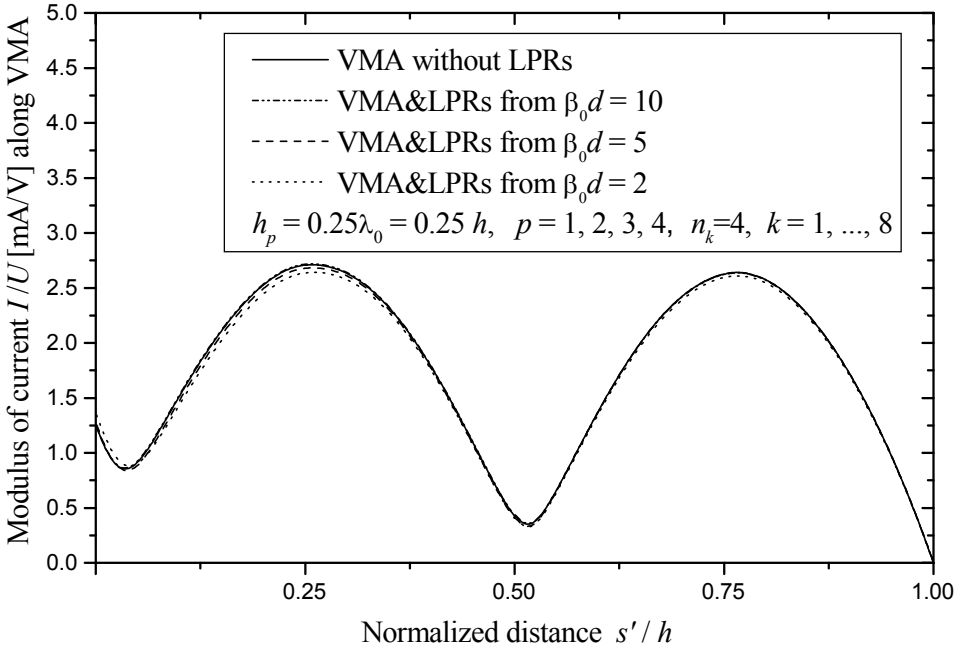

Fig. 4 – *Modulus of* I/U *along* VMA, *for* $h = \lambda_0$.

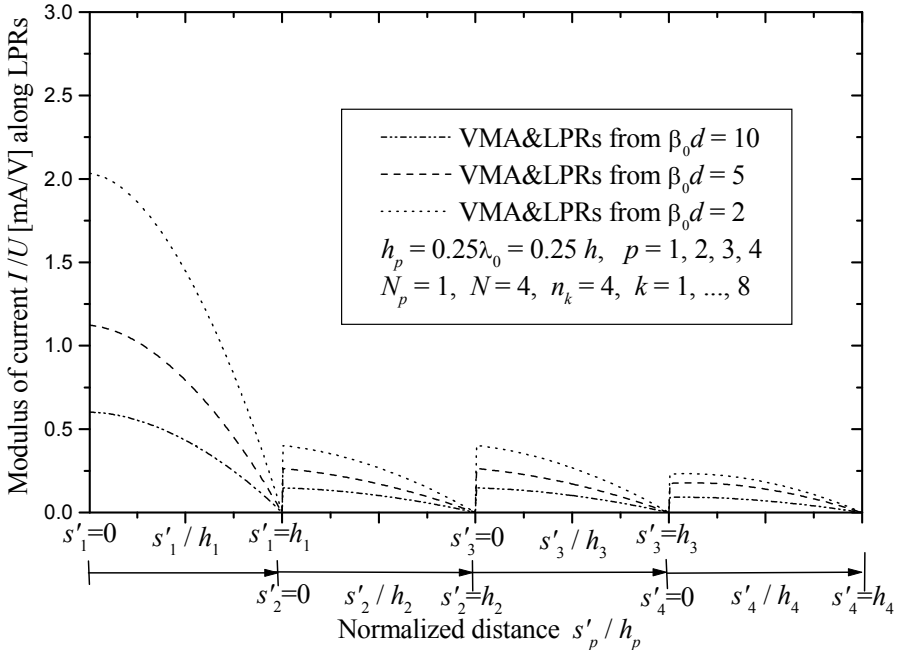

Fig. 5 – *Modulus of* I/U *along* LPRs*, for* $h = \lambda_0$.

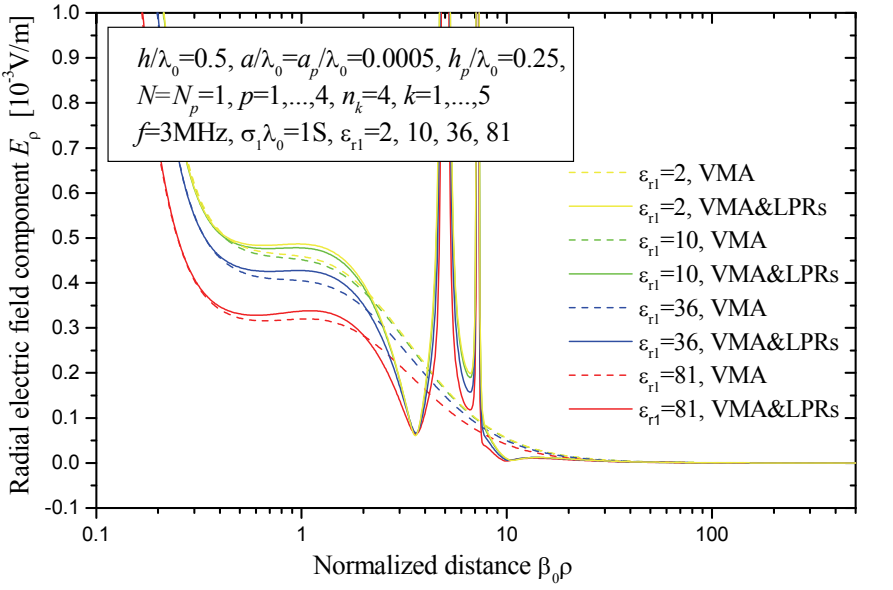

Fig. 6 – *Radial electric field component along the y-axis.*

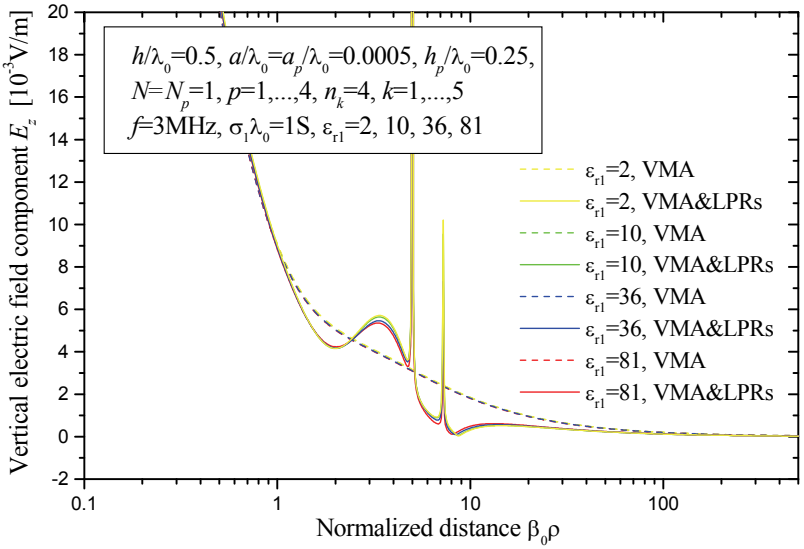

Fig. 7 – *Vertical electric field component along the y-axis.*

4 Conclusions

Current distributions along VMA and LPRs are determined in the frequency domain in the case of a lightning discharge into loss ground in the vicinity of vertical LPRs. VMA and LPRs are treated as a unique problem for boundary conditions. For obtaining unknown current distributions, approximated by polynomials, the System of integral equations of two potentials is solved numerically by the Point Matching Method. After that the input impedance of the VMA-LPRs system is determined and also the grounding impedance.

Loss half-space influence is taken into account using the new Two-image approximation (TIA) of the Sommerfeld integral kernel. Besides simplicity and generality the proposed TIA has good accuracy in a wide range of distances from VMA, i.e. in the near and far field as well. It can be very useful for solving the Sommerfeld integral numerically without limitations for ground parameters, as they can take values $\varepsilon_{r1} \in [1,81]$ and $\sigma_1 \in [0,\infty)$.

After applying the proposed procedure and determining the electromagnetic field from the VMA-LPRs system in the frequency domain, Fourier transform can be applied for obtaining LEMF in the time domain.

5 References

[1] V.A. Rakov, M.A. Uman: Review and Evaluation of Lightning Return Stroke Models Including Some Aspects of Their Application, IEEE Trans. on Electromagnetic Compatibility, Vol. 40, No. 4, Nov. 1998, pp. 403-426.

[2] V. Javor, P.D. Rancic: Application of One Suitable Lightning Return-Stroke Current Model, Proceedings of Full Papers, Int. Symposium on EMC Europe 2006, Barcelona, Sept. 2006, pp. 941-946.

[3] C. Yang, B. Zhou: Calculation Methods of Electromagnetic Fields Very Close to Lightning, IEEE Trans. on EMC, Vol. 46, No. 1, Feb. 2004, pp. 133-141.

[4] M.A. Uman, D.K. Mc Lain, R. J. Fischer, A.P. Krider: Electric Field Intensity of the Lightning Return Stroke, J. Geophys. Res., No.78, 1973, pp. 3523-3529.

[5] A. Shoory, R. Moini, H. Sadeghi, V.A. Rakov: Analysis of Lightning-Radiated Electromagnetic Fields in the Vicinity of Lossy Ground, IEEE Trans. on Electromagnetic Compatibility, Vol. 47, No. 1, Feb. 2005, pp. 131-145.

[6] A.N. Sommerfeld: Über die Ausbreitung der Wellen in der Drahtlosen Telegraphie, Ann. der Physik, Vol. 28, 1909, pp. 665-736.

[7] M.P. Rancic, P.D. Rancic: Vertical Dipole Antenna above a Lossy Half Space: Efficient and Accurate Two-Image Approximation for the Sommerfeld Integral, CD Proceedings of EuCAP 2006, Nice, Nov. 2006, Paper No. 121 (Ref. No. 362128).

[8] P.D. Rancic, V. Javor: New Two-Image Approximation of Sommerfeld's Integral Kernel in Calculation of Electromagnetic Field of Vertical Mast Antenna in Frequency Domain, Book of Abstracts, 2nd Int. Symposium on Lightning Physics and Effects, European COST Action P18, Vienna, April 2007, pp. 48-49.

[9] V. Javor, P.D. Rancic: Vertical Monopole Antenna Model of the Lightning Discharge Current: Two-Image Approximation of Sommerfeld's Integral Kernel, 16th Conference on the Computation of Electromagnetic Fields COMPUMAG 2007, PD4-22, Aachen, June 2007.

[10] V. Javor, P.D. Rancic: Vertical Mast Antenna above Real Ground: Ground Wave Electric Field, (in Serbian), 51st ETRAN Conference, Herceg Novi-Igalo, June 2007.

[11] P.D. Rancic: Contribution to Linear Antennas Analysis by New Forms of Integral Equations of Two Potentials," 10th Conference on the Computation of Electromagnetic Fields COMPUMAG'95, Berlin, July 1995, pp. 328-329.

[12] R.F. Harrington: Field Computation by Moment Methods, Macmillan, NY, Sec. 6.2, New York, 1968.

[13] B.D. Popovic: Polynomial Approximation of Current along Thin Symmetrical Cylindrical Dipoles, Proceedings of IEE, Vol. 117, No. 5, May 1970, pp. 873-878.

[14] P.D. Rancic, J.V. Surutka, M.I. Kitanovic: The Influence of Finite Ground Conductivity on Characteristics of a Vertical Mast (Monopole) Antenna with Elevated Feeding, Int. Symp. on EMC, L1-2, Rome, Sept. 1996, pp. 427-432.

[15] V.V. Petrovic: ETF Belgrade, Department of Theoretical Electrical Engineering, private communication, 2005.

[16] A.R. Djordjevic, M.B. Bazdar, V.V. Petrovic, D.I. Olcan, T.K. Sarkar, R.F. Harrington: AWAS for Windows, Version 2.0, Analysis of Wire Antennas and Scatterers - Software and User's manual, Artech House, 2002.